Numerical model of the Tikitere geothermal system

Melissa Baars[1,2], Theo Renaud[1], Jeremy Riffault[1], Michael O'Sullivan[1], John O'Sullivan[1], Michael Gravatt[1], Ken Dekkers[1], Michel Speetjens[2]

[1]Geothermal Institute, University of Auckland, 70 Symonds Street, Grafton, Auckland, 1010, New Zealand

[2]Eindhoven University of Technology, Eindhoven, Netherlands

m.osullivan@auckland.ac.nz

Keywords: *Tikitere, AUTOUGH2, Waiwera, ITOUGH2*

ABSTRACT

The Tikitere geothermal field is one of the 21 high-enthalpy geothermal fields in the Taupo Volcanic Zone (TVZ) in New Zealand. The field is renowned for the tourist attraction Hell's Gate, which consists of many natural geothermal surface features. Based on geoscientific data from the open-source literature, a conceptual model was set up in Leapfrog Geothermal. A corresponding natural state reservoir model was then set up and calibrated using temperature and heat flux data from fourteen thermal areas. The calibrated numerical model matches the higher temperatures at the locations of some of the surface thermal features but does not match the estimated heat flows.

1. INTRODUCTION

1.1 Context

The Tikitere geothermal field is one of the 21 high-enthalpy geothermal fields in the Taupo Volcanic Zone (TVZ) in North Island of New Zealand (Simpson and Bignall, 2016). The TVZ stretches from Mount Ruapehu in the south to the Bay of Plenty in the north. Under the TVZ, the oceanic Pacific plate is being subducted below the continental Australian plate, at a rate of up to 15mm per year (Bertrand et al., 2022). This produces a thin continental crust caused by intra-arc rifting. As a result, magma from the mantle is located closer to the crust and creates much volcanic and geothermal activity in the area. Due to the large number of faults and fractures, heat is discharged at the surface in geothermal areas in the form of geysers, hot springs and mud pools (Simpson and Bignall, 2016).

Figure 1 shows the location of the Tikitere geothermal field, an area of approximately 12 km^2 (Gordon, 2002) close to Lake Rotorua in the west and Lake Rotoiti in the north. The area is positioned in a graben, lowered by tectonic subsidence between two parallel normal faults (Manville et al., 2007).

Tikitere is renowned for the tourist attraction Hell's Gate, which consists of many natural geothermal surface manifestations. Previous researchers have pointed out that Tikitere has a large potential for geothermal exploitation (Espola, 1974; Simpson and Bignall, 2016). Dickinson, 1971 estimated the natural output from Tikitere at 120 MW (heat) relative to a mean annual temperature of 12°C. The local authority, the Bay of Plenty Regional Council, has classified Tikitere as a "conditional development system" (Scott and Scholes, 2021), which indicates that there is a potential for extractive use. However, to date, no deep wells have been drilled in the Tikitere area (Lawless et al., 2020).

Two caldera structures are located close to the Tikitere geothermal field: the Rotorua and the Okataina calderas. In Figure 1, the margins of these caldera structures are indicated. In a recent study on the Okataina Volcanic Complex (Pearson-Grant et al., 2022), it was found that the caldera structure has some influence on the local geothermal upflow. For the Tikitere geothermal system, the results of Pearson-Grant et al. (2022) suggest that "the topographic lows associated with caldera margins are primarily responsible for localized geothermal upflow around the margins of the OVC".

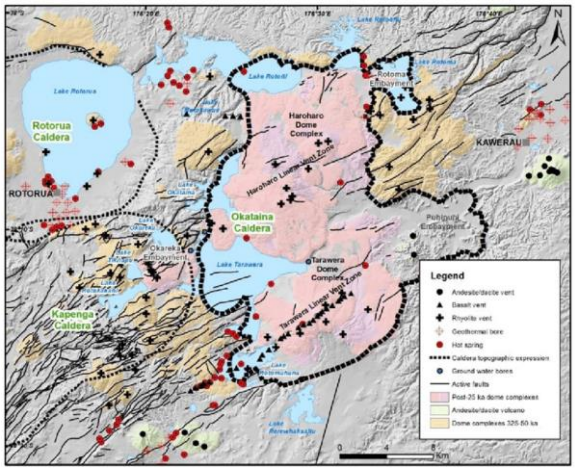

Figure 1: Caldera structures close to the Tikitere area (Massiot et al., 2020).

1.2 Surface Manifestations

Many surface manifestations are present in the Tikitere area, as shown in Figure 2. Dickinson (1971) identified fourteen thermal areas and five streams, with an estimated total area of 248,000 m^2 and a total heat flow of 120.5 MW relative to 12°C.

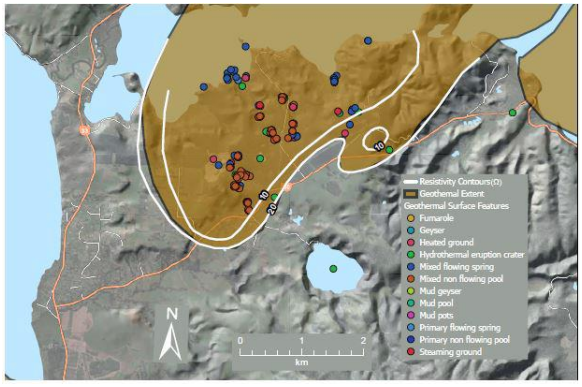

Figure 2 : Geothermal extent and surface features in the Tikitere area (Simpson and Bignall, 2016)

ISSN 2703-4275

The thermal areas consist of altered steaming ground with fumaroles, (boiling) springs, mud pools and streams (Simpson and Bignall, 2016). From the measured natural heat flow, 98 MW is related to evaporation, ground surface conduction and convection from pools. The other 22.5 MW is the result of evaporation and direct discharge of streams.

An overview of the individual surface features is presented in the Appendix. Espola (1974) identified >160 pools and springs within or close to the previously mentioned thermal areas, of which 38 were analyzed in detail. Temperatures in the pools and springs varied from 33°C up to 95.5°C. Besides these areas, hot springs are also believed to occur on the bed of Lake Rotoiti (Espola, 1974).

2. CONCEPTUAL MODEL

2.1 Geological model

Due to the unavailability of well data, the surface contacts between formation were modeled based on cross-sections and geological maps of the area (Espola, 1974; Alcaraz, 2014). First, these maps were imported into Leapfrog and then georeferencing was applied to ensure that all maps were imported with the UTM zone 60 (south) as the coordinate system.

Table 1: Formation chronology in the Tikitere model (Leonard et al., 2010)

	Formation Chronology	Surface type	Map symbol
Young	Sediment	Deposit	Q1a, IQK, Q3a
	Rotokawau	Intrusion	Q1z
	Haroharo subgroup	Erosion	Q1o, Q2o, Q3o
	Post-caldera rhyolithic domes	Intrusion	mQr
	Rotoiti/Mangaone Ignimbrite	Erosion	Q3z, Q4z
	Pre-caldera rhyolithic domes	Intrusion	mQr
	Mamaku Ignimbrite	Deposit	Q7u
	Haparangi 1	Intrusion	mQz, eQz
	Pokopoko Ignimbrite	Deposit	Q8z
	Pre-mamaku formation	Deposit	na
Old	Basement	Deposit	na

Conversion of coordinates was done using the LINZ conversion tool (LINZ, n.d.). Subsequently, GIS lines were drawn to digitize the lithologies and faults that are visible at the surface. The lithological surfaces were built up by adding each surface contact as a deposit, intrusion or erosion. When deposit surfaces are created, the layer appears conformably on top of older deposits without affecting them (Leapfrog, n.d.). Erosion surfaces remove part of the older deposit and form a new layer on top of the older deposit, while intrusion surfaces remove all the existing material of (multiple) older lithologies (Figure 3).

In Table 1, an overview of the formation chronology and their surface type is presented.

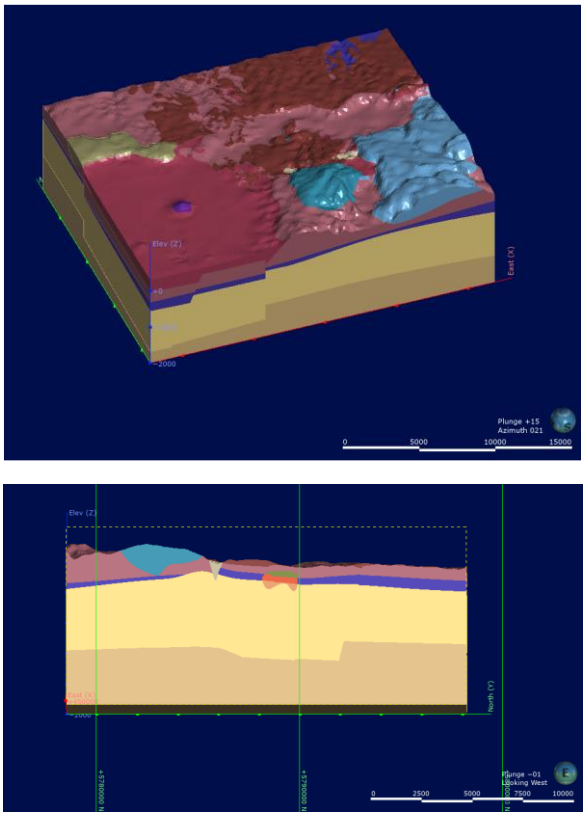

Figure 3: 3D view and cross-section of the digital conceptual model.

2.2 Clay cap interpretation

The location of the clay cap can be deduced from electrical resistivity data. A simplified map of the Tikitere resistivity contour (MacDonald 1974) was used.

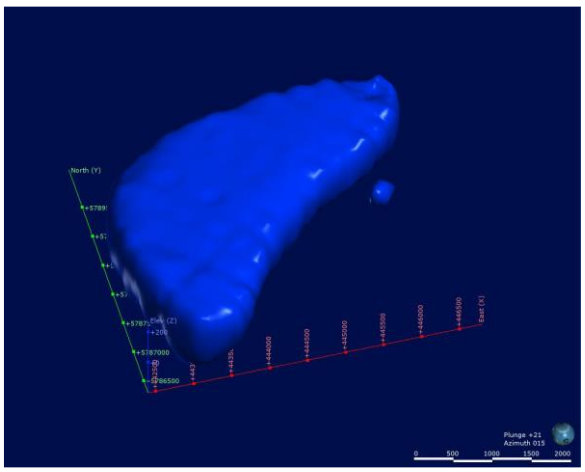

Figure 4: Inferred volume of the clay cap.

Both the 10 and 20 Ωm contours were digitized and then, based on descriptions of the geothermal system (Sheppard and Lyon, 1979; Simpson and Bignall, 2016), an estimation was made of the depth of the clay cap. A digital Leapfrog model was created using the radial basis function (RBF) interpolation of the 10 and 20 Ωm contours. An output

Proceedings 45th New Zealand Geothermal Workshop
15-17 November, 2023
Auckland, New Zealand
ISSN 2703-4275

volume for the clay cap was extracted based on the < 10 Ωm iso-surface, as presented in Figure 4.

2.3 Extent of the system

In Figure 5, resistivity contour data for the Tikitere geothermal field near the surface are shown (Macdonald, 1974). A simplified version of this map, created by Simpson and Bignall (2016), is presented in Figure 6. The maps show that the 10 Ωm contour stretches in a northeast direction, extending below Lake Rotoiti. The contour is approximately 4.8 km long and 2.3 km wide. The depth of the resistivity contour is not specified in either of the maps. Therefore, additional data are needed to estimate the depth of the clay cap.

Figure 5: Resistivity of the Rotorua geothermal region, including Tikitere (Macdonald, 1974). Coordinates are presented in North Island National grid (yards).

According to Sheppard & Lyon (1979), the Tikitere geothermal field consists of a steam condensate zone up to 400 m depth, overlaying a two-phase boiling chloride reservoir up to 3 km in depth. The permeability of the condensation zone is poor, due to silicification of Rotoiti Ignimbrite (Espola, 1974; Sheppard and Lyon, 1979). Temperatures in the reservoir at 3 km depth reach just over 250°C. Deep MT resistivity data from the Tikitere geothermal field (Bertrand et al., 2022, as shown in Figure 7) show an anomaly of low (< 10Ωm) resistivity up to a depth of 10 km.

In Figure 6, a low resistivity anomaly is shown 5 km north of Tikitere, corresponding to the Taheke geothermal field. Some hot surface features are found in Taheke (Espola, 1974). Researchers have long debated whether the Tikitere and Taheke fields are two discrete systems, or one single system, connected at depth (Macdonald, 1974; Espola, 1974; Scott and Scholes, 2021).

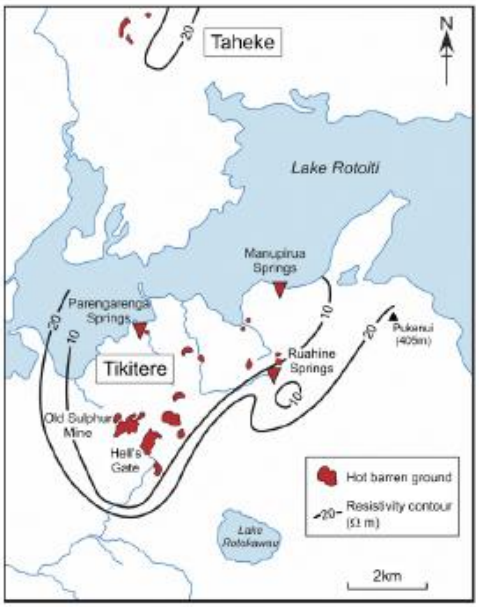

Figure 6: Simplified map of the resistivity contours in the Tikitere area (Simpson and Bignall, 2016), based on the resistivity contour survey of (Macdonald, 1974). A small correction needs to be made to the length scale in the right-bottom: the 2 km bar represents approx. 1.2 km.

The MT resistivity profiles in Figure 7 (Bertrand et al., 2022), show evidence for a single heat plume at a large depth (>5 km), supporting the likelihood of a connection between the two fields.

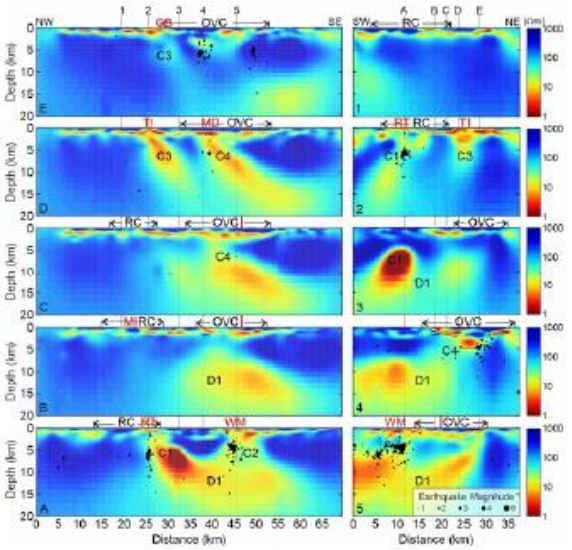

Figure 7: Cross-sections through the 3-D resistivity model (Bertrand et al., 2022). The Tikitere geothermal field is marked as TI. The low resistivity plume of the Tikitere geothermal field is marked as C3.

The direction of the MT resistivity plume of Figure 7 seems to align with the face dip of the Mourea Fault (Fault C), which might be the main pathway for the deep upflow toward both geothermal fields. However, drilling data are needed to confirm that this is the case. Currently, the Taheke geothermal field is being investigated for future

Proceedings 45th New Zealand Geothermal Workshop
15-17 November, 2023
Auckland, New Zealand
ISSN 2703-4275

geothermal production. In 2020, the energy company Eastwood Energy announced a collaboration with Taheke 8c and Incorporated Land Blocks Incorporation, for the development of a 25 MWe geothermal power station (Bay of Plenty Regional Council, 2020). In 2021, deep exploration wells were drilled at Taheke, but no data are publicly available. Due to time constraints of this research and the uncertainty of the exact relation between the two fields, it was decided to focus solely on modelling the Tikitere geothermal field.

3. NUMERICAL RESERVOIR MODEL

3.1 Grid design

The grid is 14 km by 14 km and uses two refinement steps, going from 500m x 500m blocks at the side, to 250m x 250m blocks around the 10 Ωm resistivity contour and 125m x 125m blocks near the surface manifestations. Figure 8 shows a 2-D plan view of the grid. In the z-direction, the grid contains 56 layers. They are 500 m thick at the bottom of the model, but the layer thickness decreases to 25 m at the surface to allow the topography and the water table to be well represented. The reservoir model contains a total of 50,397 blocks.

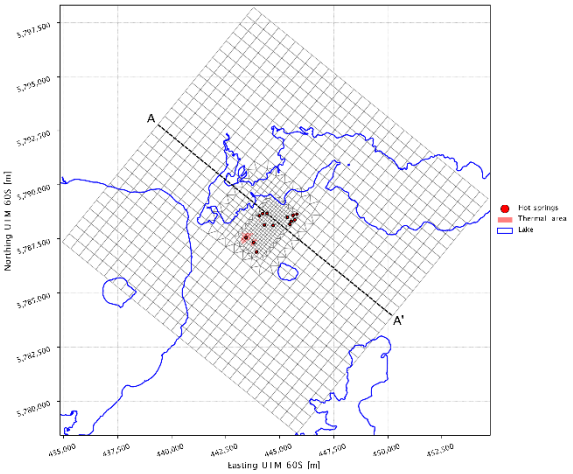

Figure 8: Plan view of model grid. Coordinates are given in UTM zone 60 (south).

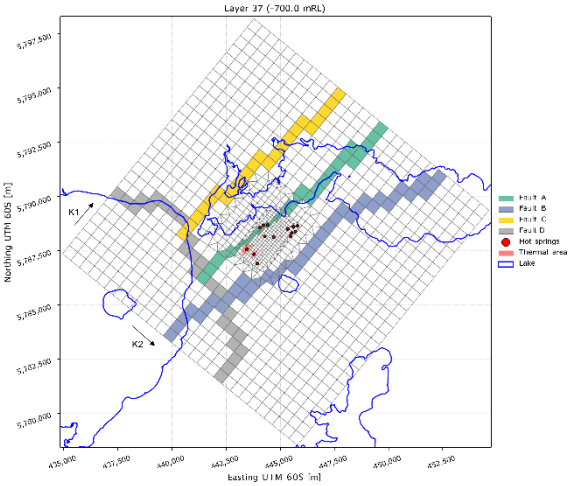

Figure 9: Plan view of the faults in the Tikitere model. Magnitudes of K1 permeabilities are coloured.

Four faults are included in the model (see Figure 9), namely: Inferred Fault (Fault A), Moose Lodge Fault (Fault B) and Mourea Fault (Fault C), all trending in an SW-NE direction and the Rotorua caldera (Fault D) runs from NW to SE. The k1 permeability direction is aligned with the dominant direction of Faults A, B and C and the k2 permeability direction is aligned with the direction of Fault D.

3.2 Boundary conditions

Sides

The reservoir model uses closed boundary conditions at the sides.

Base

At the base of the model a background heat flux boundary condition was set to 80 mW/m^2.

Also, mass source terms were added in the bottom layer to simulate a deep upflow at the base of the model. Based on the estimated natural heat output of the thermal areas (98 MW) (Macdonald, 1974) and the estimated temperature of over 250 °C at ~3km depth (Sheppard and Lyon, 1979), it was decided to initially set a total flow of 80 kg/s with a temperature of 270 °C (an enthalpy of 1185 kJ/kg, giving a heat input of 94.8 MW). The upflow was added in the blocks where the Mourea fault (Fault C) intersects with the Inferred fault (Fault A).

During manual calibration, and the later experiments with automatic calibration with iTOUGH2, the magnitude and location of the deep upflow was allowed to vary.

Surface

At the surface blocks rainfall is injected based on the average values for Lake Rotoiti (World Weather Online, 2022).

The top boundary was fixed at atmospheric pressure (1 bar) and temperature (12°C). For the blocks representing the beds of Lake Rotoiti and Lake Rotorua, different boundary conditions were set. The pressure at these blocks were set to correspond to the hydrostatic pressure at the bottom of the lake and a temperature of 12°C was set. No rainfall was injected in the lake blocks.

3.3 Permeability structure

For the Tikitere model, each block was assigned a specific five-character, rock type identifier based on a standard naming convention. In Table 2, an overview of the different rock types is presented. An example of a rock type identifier is: BC001. The first character indicates the type of formation, which is the basement (B) in this case. The second indicates the presence of a fault (C = the Mourea Fault). The third character indicates a second fault that intersects with the first fault (0 = none). The fourth character indicates the presence of the alteration, which is not present (0) in this case. The fifth character represents the location of the rock in the geothermal field (1 = inside the geothermal reservoir).

The initial permeability on a NW-SE slice through the model is shown in Figure 10. The cap (altered zone) is shown as dark blue.

Proceedings 45th New Zealand Geothermal Workshop
15-17 November, 2023
Auckland, New Zealand
ISSN 2703-4275

Table 2: Naming convention of the rock types in the Tikitere model.

1. Formation	2. 1st fault	3. 2nd Fault	4. Altered	5. Version
A = Haparangi 1	0 = none	0 = none	0 = no	0 = surface
B = Basement	A = Inferred Fault	A = Inferred Fault	A = yes	1 = inside reservoir
H = Haroharo group	B = Moose Lodge Fault	B = Moose Lodge Fault		2 = outside reservoir
I = Rotoiti	C = Mourea Fault	C = Mourea Fault		3,4,5, …= other versions
K = Rotokawau	D = Rotorua Caldera	D = Rotorua Caldera		
M = Mamaku				
N = Pre-mamaku				
P = Pokopoko				
R = Post-caldera rhyolite				
S = Sediment				
T = Pre-caldera rhyolite				

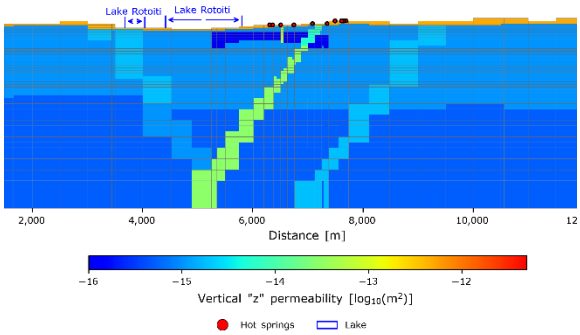

Figure 10: Cross-section of Model 4, indicating the vertical permeability k3 of the rock formations. In this model, the vertical permeability of Fault A was 50 mD.

4. RESULTS

4.1 Modelling procedure

The unavailability of deep well data makes the standard natural state calibration procedure of matching temperature profiles impossible. Instead, a qualitative assessment of the temperature distribution and a quantitative assessment of temperatures and heat flux of the surface features were used for model calibration.

4.2 Permeability of Fault A

In the first series of numerical experiments the vertical permeability of Fault A was increased from 7, to 10, 30 and 50 mD (listed as Models 1, 2, 3, 4 in Table 3). Even for Model 4, with k3=50 mD, the calculated heat flux from the 14 thermal areas was only 7.4 MW, an order of magnitude less than the value of 98 MW given in the literature.

Table 3: Model parameters.

Model	K3 permeability in Fault A (mD)	Total deep upflow (kg/s)
1	7	80
2	10	80
3	30	80
4	50	80
5	50	160

A plan view of surface temperature for Model 4 (k3= 50 mD in Fault A) is given in Figure 11**Error! Reference source not found.**. The surface temperatures in the Tikitere area are too low and those to the NW, under Lake Rotoiti, are too high.

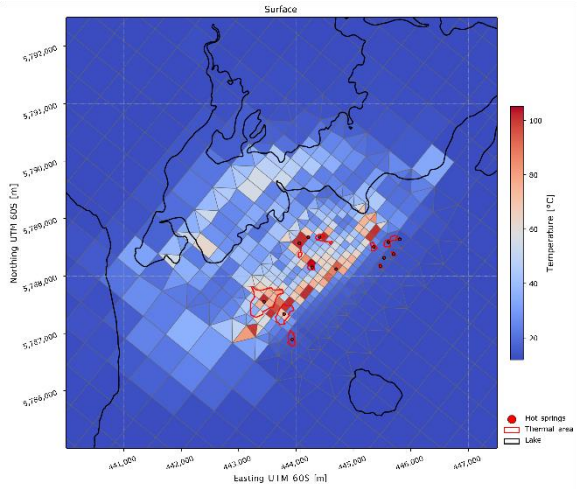

Figure 11: Plan view of the surface temperatures reached for Model 4. The outlines of Lake Rotorua and Lake Rotoiti are drawn in black.

4.3 Magnitude of upflow

Next, the influence of the upflow mass flow rate on the surface temperatures and heat flux was explored. The mass upflow was doubled to 160 kg/s. This model is called Model 5 (see Table 3). The vertical permeability of Fault A is kept constant at 50 mD.

Proceedings 45th New Zealand Geothermal Workshop
15-17 November, 2023
Auckland, New Zealand
ISSN 2703-4275

In Figure 12, the NW-SE cross-section of temperature distribution in the natural state for Model 5 is presented.

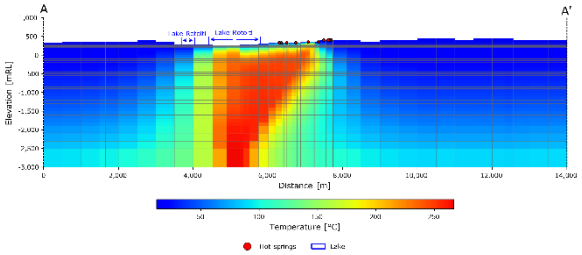

Figure 12: Cross-section of temperature distribution in Model 5 (k3= 50mD in Fault A, hot upflow of 160kg/s).

The results are qualitatively reasonable but as shown below the surface temperatures and heat flows are still not well matched to the data. In Table 4, the surface temperature and heat flux results for Model 4 and Model 5 are shown. As expected, the results show that a higher total mass flow leads to higher temperatures and heat flow values in all thermal areas. However, for most of the thermal areas the heat flow is still too small. The exceptions are thermal areas 4 and 6, for which the heat flow has become too large.

Some of the surface temperatures are too hot (e.g., Areas 3, 4,5, 7, 8 - see Table 4) even though the heat flow at the same locations is too small.

Table 4: Surface temperature and heat flow in the thermal areas at Tikitere.

	Data		Model 4		Model 5	
Area	**T (°C)**	**Heat (MW)**	**T (°C)**	**Heat (MW)**	**T (°C)**	**Heat (MW)**
1	45-100	4.18	15.8	0.021	26.1	0.077
2	31.5-113	30.16	91.4	0.248	101.0	0.970
3	31.5-86	10.43	101.8	1.951	102.2	3.108
4	56	0.19	105.5	1.930	105.9	2.973
5	52.5-98	13.4	30.9	0.110	100.6	0.700
6	No data	0.08	101.2	0.825	101.4	1.463
7	40-92	1.97	101.5	0.636	101.8	1.331
8	81-85	3.93	101.3	1.255	101.6	2.120
9	60	1.49	14.8	0.006	17.9	0.013
10	72	2.04	15.8	0.005	20.2	0.010
11	82.5	3.05	15.5	0.004	19.6	0.009
12	68.2	10.17	31.9	0.062	49.7	0.118
13	No data	0.22	14.1	0.020	20.3	0.080
14	33-83	16.71	101.0	0.348	101.2	0.628
Total		98.02		7.4		13.6

5. INVERSE MODELLING

To try to improve the calibration of the model we applied the automatic calibration (inverse modelling) software iTOUGH2 (Finsterle & Pruess, 1999; Finsterle, 2007. The temperatures at 21 surface blocks were used as the observations to be matched and the adjustable model parameters used were the magnitude of the deep upflow in 123 blocks and the k1, k2, k3 permeabilities of 60 rock types giving a total of 303 adjustable parameter.

We used temperatures given by Espola (1974) or Meza (2004) for 60 of the 68 identified individual surface features at Tikitere. In many cases several surface features are located in the same model block and only 21 surface blocks were used for observations. For multiple surface features in one block an average temperature was used as the observation.

In addition, the mass flows at the 14 hot spring areas (multiple blocks in some cases) were added as observations to be matched. These mass flows have not been measured and were calculated approximately from the heat flows given in Table 4 by assuming mass flow to the surface is 80% water and 20% steam.

For manual calibration upflow was applied only in blocks at the intersection of Faults A and C at the base of the model. For the iTOUGH2 simulations the possibility of upflow at the base of Fault B is also included (see Figure 10).

The results to date are disappointing with no significant improvement of the match to surface temperatures and mass outflows achieved by iTOUGH2. This may mean that more heterogeneity is required in the permeability structure to allow a better match to the surface features.

6. CONCLUSION

A digital conceptual model of Tikitere has been built based on open-source data and using the Leapfrog software. This was used to construct a numerical model that was used to simulate the natural state of Tikitere. A qualitatively reasonable distribution of surface temperatures was obtained but quantitatively the model temperatures do not accurately match the data.

Also, the overall heat flow coming out of the thermal areas in the model is too small. The data indicate a total heat flow of 98 MW from the 14 thermal areas whereas the best model (Model 5) gives only 13.6 MW. Model 5 has a deep upflow at its base of 190 MW most of which must be outflowing at the surface outside the thermal areas, indicating that the flow paths in the model are not yet correct.

So, this study was a useful first step in understanding and modelling the Tikitere geothermal field but more work on both the conceptual model and the numerical model is required to improve the representation of the surface features at Tikitere.

REFERENCES

Alcaraz, S. (2014). 3-D Geological model of Rotorua (tech. rep. No. 289). Institute of Geological and Nuclear Sciences Limited. Taupo.

Bay of Plenty Regional Council. (2020). Draft Change 5 (Kaituna River) to the Bay of Plenty Regional Policy Statement. https://atlas.boprc.govt.nz/api/v1/edms/document/A3649662/content

Bertrand, E. A., Kannberg, P., Caldwell, T. G., Heise, W., Constable, S., Scott, B., Bannister, S., Kilgour, G., Bennie, S. L., Hart, R., & Palmer, N. (2022). Inferring the magmatic roots of volcano-geothermal systems in the Rotorua Caldera and Okataina Volcanic Centre from magnetotelluric models. Journal of Volcanology and Geothermal Research, 431 (August).

Dickinson, D. (1971). The Natural Heat Output of the Tikitere Thermal Area. Technical Report, Geophysics Division, Department of Scientific and Industrial Research. Wellington.

Espola, O. (1974). Geology and Hot Springs of Tikitere and Taheke Hydrothermal Fields, Rotorua, New Zealand

Finsterle, S. & Pruess, K. (1999) Automatic Calibration of Geothermal Reservoir Models through Parallel Computing on a Workstation Cluster. *Proc.*, 24th Workshop on Geothermal Reservoir Engineering. Stanford University, Stanford, CA, USA.

Finsterle, S. (2007) *iTOUGH2 User's Guide*, Report LBNL-40040, Earth Sciences Division Lawrence Berkeley National Laboratory, University of California, Berkeley, CA 94720, USA. 137 p.

Gordon, D. (2002). Groundwater Resources of the Bay of Plenty. Technical Report, Environment Bay of Plenty Regional Council, Whakatane.

Lawless, J., Van Campen, B., & Randle, J. (2020). Future Geothermal Generation Stack. Technical Report, Lawless Geo-Consulting. https://www.mbie.govt.nz/assets/future-geothermal-generation-stack.pdf

Leapfrog. (n.d.). Contact Surfaces. https://help.seequent.com/Geo/4.3/en-GB/Content/geo-models/contact-surfaces.htm#deposits-and-erosions

Leonard, G.S., Begg, J.G., & Wilson, C.J. (2010). Geology of the Rotorua area. Lower Hutt, New Zealand. Technical Report, Department of Scientific and Industrial Research New Zealand.

Macdonald, W. (1974). Geophysical investigation of the Rotorua Geothermal District. Technical Report, Department of Scientific and Industrial Research.

Manville, V., Hodgson, K., & Nairn, I. (2007). A review of break-out floods from volcanogenic lakes in New Zealand. New Zealand Journal of Geology and Geophysics, 50(2), 131–150.

Meza, P. (2004). The Natural Thermal Feature of the Tikitere geothermal field and the characteristics of its surface geology. University of Auckland.

Pearson-Grant, S. C., Miller, C. A., Carson, L. B., Bertrand, E. A., & Leonard, G. S. (2022). Influences on geothermal circulation in the Okataina Volcanic Centre, New Zealand. Journal of Volcanology and Geothermal Research, 432 (November), 107705.

Scott, B., & Scholes, P. (2021). Bay of Plenty, Geothermal Systems - The Science Story. Technical Report by GNS Science for Bay of Plenty Regional Council.

Sheppard, D., & Lyon, G. (1979). The chemical and isotopic composition of water and gas discharges from the Tikitere and Taheke geothermal fields, New Zealand. Technical Report, Chemistry Division, DSIR.

Simpson, M.P., & Bignall, G. (2016). Undeveloped high-enthalpy geothermal fields of the Taupo Volcanic Zone, New Zealand. Geothermics, 59, 325–346.

ISSN 2703-4275

Appendix. List of 68 identified surface features at Tikitere

id no.	location	name	area (m2)	depth (m)	Temp. (deg C) (Hell's gate maps)	Temp. (deg C) Meza (2004)	Temp. (deg C) Espola (1974)	pH	Elev. (masl)	x (east) (UTM zone 60)	y (north) (UTM zone 60)	Type	Flow rate (L/s)	Thermal area	Source	Temp. selected	Model block
1	Hell's gate	Outflow LLM		?				2.2	320.38	443967.1	5786871.5	Stream	3	1	Meza (2004)		
2	Hell's gate	Devil's Bath	108	6	45	51.4		2.3	319.05	443948.0	5786848.8	Non flowing pool	0	1	Hell's gate tourist map	45	apv15
3	Hell's gate	Ink pots		20	76	90		2	319.60	443937.2	5786868.4	Non flowing pool	0	1	Hell's gate tourist map	76	apv15
4	Hell's gate	Huritini	346	15	42	40.9	54	2.2	319.67	443956.5	5786860.7	Non flowing pool	0	1	Hell's gate tourist map	42	apv15
5	Hell's gate	Hell's gate	611	25	45	40.3	52	2	320.42	443940.8	5786886.8	Non flowing pool	0.5	1	Hell's gate tourist map	45	apv15
6	Hell's gate	Baby Adam		1	68	80.1		6	320.93	443957.0	5786893.1	Non flowing pool		1	Hell's gate tourist map	68	apv15
7	Hell's gate	Sulphur bath	241		74	46.6		1.8	321.57	443952.3	5786910.3	Non flowing pool	0	1	Hell's gate tourist map	74	apv15
8	Hell's gate	Steaming fumaroles						?	323.25	443912.0	5786960.9	Fumarole		1	Hell's gate tourist map		
9	Hell's gate	Inferno pools	1068		60.5	62.8		2.5	323.99	443907.3	5786978.8	Non flowing pool	0.5	1	Hell's gate tourist map	60.5	aqr15
10	Hell's gate	Sodom & Gomorrah			100			?	324.96	443906.2	5787000.3	Non flowing pool		1	Hell's gate tourist map	100	aqo15
11	Hell's gate	The infants						?	324.78	443930.0	5786988.6	Non flowing pool		1	Hell's gate tourist map		
12	Hell's gate	Spraying pools			84			2.5	325.35	443928.2	5787001.7	Heated ground		1	Hell's gate tourist map	84	aqo15
13	Hell's gate	Kakahi falls			40			?	331.60	443811.2	5787117.4	Waterfall	3	2	Hell's gate tourist map	40	aqp15
14	Hell's gate	Map of Australia	249		36	24.7		3.8	333.86	443781.2	5787207.1	Flowing spring	0.5	2	Hell's gate tourist map	36	api15
15	Hell's gate	Crystal valley						?	336.96	443714.7	5787234.7	Deposits	0	2	Hell's gate tourist map		
16	Hell's gate	Devil's Cauldron	1412		110	55.2		?	339.98	443694.1	5787260.1	Non flowing pool	1	2	Hell's gate tourist map	110	apj14
17	Hell's gate	Mud volcano						-	339.49	443768.1	5787383.3	Mud volcano	0	2	Hell's gate tourist map		

ISSN 2703-4275

18	Hell's gate	Steaming cliffs pool			113	88.8	91	?	340.86	443790.2	5787490.0	Flowing spring	1	2	Hell's gate tourist map	113	aro14
19	Hell's gate	Cooking pool			76	75.1		6.2	344.66	443883.2	5787421.0	Non flowing pool	0	2	Hell's gate tourist map	76	arn14
20	Hell's gate	Medicine lake			54	35			347.92	443941.7	5787414.0	Non flowing pool		2	Hell's gate tourist map	54	arn14
21	Hell's gate	The Big One	4011			44.6	45	3	338.47	443794.6	5787271.9	Non flowing pool	1	2	Meza (2004)	44.6	arm14
22	Hell's gate	Hot Sulfur Lake	3939			42.7		2.5	342.53	443832.8	5787432.1	Non flowing pool	1	2	Meza (2004)	42.7	aro14
23	Hell's gate	Small Hot Sulfur Lake	1061			59.9		3	341.58	443788.6	5787444.7	Non flowing pool	0.5	2	Meza (2004)	59.9	aro14
24	Hell's gate	N. Green Pool				58.5		5	344.88	443885.9	5787433.0	Non flowing pool	0	2	Meza (2004)	58.5	arn14
25	Hell's gate	Teeth Pool	566			31.5		3.5	335.02	443754.6	5787210.7	Flowing spring	3	2	Meza (2004)	31.5	api15
26	Hell's gate	Mud Volcano Lake	3936			52.9		6	338.07	443738.2	5787360.1	Non flowing pool	0.5	2	Meza (2004)	52.9	arp14
27	Hell's gate	Cooking pot				35		6.2	345.29	443896.1	5787412.3	Non flowing pool	0	2	Meza (2004)	35	arn14
28	Hell's gate	spring 7					75	3.37	339.48	443738.0	5787417.9	Non flowing pool		2	Espola (1974)	75	arp14
29	Old Sulfur Mine	Pool 1	50			86	60	5.41	334.32	443743.9	5787716.8	Flowing spring	1	3	Meza (2004)	86	ate15
30	Old Sulfur Mine	Pool 2	100			80			332.59	443726.9	5787731.3	Flowing spring	1	3	Meza (2004)	80	ate15
31	Old Sulfur Mine	Pool 3	530			53			332.50	443608.9	5787554.8	Non flowing pool		3	Meza (2004)	53	atv15
32	Old Sulfur Mine	Pool 4	670			65	74		330.84	443611.9	5787597.6	Non flowing pool	1	3	Meza (2004)	65	atv15
33	Old Sulfur Mine	Lake	7000			31.5	38		328.95	443427.0	5787574.6	Non flowing pool		3	Meza (2004)	31.5	ml15
34	Old Sulfur Mine	Pool 5				0			324.47	443508.9	5787641.6	Flowing spring	0	3	Meza (2004)		
35	Maraeroa	Maraeoroa spring 2					57	2.13	338.62	444234.4	5788141.4	Non flowing pool		4	Espola (1974)	57	asr14
36	Maraeroa	Crater							335.62	444287.9	5788182.5	Hydrothermal eruption crater		4			
37	Maraeroa	spring 22					34	2.8	343.49	444266.4	5788059.1	Flowing spring		4	Espola (1974)	34	asa14
38	Maraeroa	spring 23					63.5	2.7	346.23	444318.9	5788019.0	Flowing spring		4	Espola (1974)	63.5	asa14

Proceedings 45th New Zealand Geothermal Workshop
15-17 November, 2023
Auckland, New Zealand
ISSN 2703-4275

39	Ruahine	Pool 1				94.7	95.5	6.32	371.92	445543.2	5788532.2	Flowing spring	0	5	Meza (2004)	94.7	auf14
40	Ruahine	Pool 2				97.5	94		372.90	445596.2	5788526.8	Flowing spring	1.5	5	Meza (2004)	97.5	14-Aug
41	Ruahine	Pool 3				97.5			370.99	445604.2	5788553.3	Flowing spring	0	5	Meza (2004)	97.5	45152
42	Ruahine	Pool 4					52.5		367.36	445599.1	5788594.6	Non flowing pool	0	5	Espola (1974)	52.5	45152
43	Maraeroa	Maraeoroa spring 3					40	2	325.85	444394.4	5788692.1	Non flowing pool		7	Espola (1974)	40	asg15
44	Maraeroa	Maraeoroa spring 4					92	3.2	323.15	444594.4	5788576.9	Non flowing pool		7	Espola (1974)	92	apn15
45	Maraeroa	spring 15					85	2.4	317.84	444055.1	5788579.1	Flowing spring		8	Espola (1974)	85	aqf15
46	Maraeroa	spring 16					87	2.5	318.05	444039.0	5788573.7	Flowing spring		8	Espola (1974)	87	aqf15
47	Maraeroa	spring 18					89	2.2	327.73	444075.0	5788403.3	Flowing spring		8	Espola (1974)	89	aqd15
48	Maraeroa	spring 19					91	2.2	328.94	444051.6	5788394.3	Flowing spring	0.5	8	Espola (1974)	91	aqd15
49	Thermal area 9	spring 35					60	3.2	381.24	445688.6	5788378.4	Flowing spring		9	Espola (1974)	60	apd13
50	Papakiore Bath	spring 34					72	2.9	382.58	445526.6	5788318.5	Flowing spring		10	Espola (1974)	72	aqv13
51	Thermal area 11	spring 33					82.5	3.3	382.42	445457.8	5788176.6	Flowing spring		11	Espola (1974)	82.5	aqw13
52	Thermal area 12	spring 3					68.2	2.55	370.21	445338.3	5788505.1	Flowing spring		12	Espola (1974)	68.2	auy14
53	Thermal area 14	spring 24					83	4.95	348.41	444609.4	5788076.2	Flowing spring		14	Espola (1974)	83	asy14
54	Thermal area 14	spring 25					73	3	349.86	444638.7	5788075.1	Flowing spring	0.33	14	Espola (1974)	73	asy14
55	Thermal area 14	spring 26					33	2.9	348.20	444625.2	5788090.1	Flowing spring		14	Espola (1974)	33	asy14
56	Maraeroa	Maraeoroa spring 1					65		347.96	444665.5	5788126.0	Flowing spring		14	Espola (1974)	65	asy14
57	Rotokawau	Crater	520000	43.7	10.8				313.52	445373.8	5785943.3	Hydrothermal eruption crater		x	Pearson et al. (2011)	10.8	kl15
58	Tikitere	Explosion crater							354.55	444096.4	5787712.6	Hydrothermal eruption crater		x			
59	Parengarenga	Hot springs					68	6.8	286.31	443505.8	5788986.6	Flowing spring		x	Espola (1974)	68	agd16
60	Parengarenga	Hot springs					68	6.9	283.88	443500.8	5789012.5	Flowing spring		x	Espola (1974)	68	agd16
61	Parengarenga	Hot springs					63.8	2.6	286.20	443802.7	5788987.5	Flowing spring		x	Espola (1974)	63.8	agb16

Proceedings 45th New Zealand Geothermal Workshop
15-17 November, 2023
Auckland, New Zealand
ISSN 2703-4275

62	Parengarenga	Hot springs					68	2.5	293.08	443672.9	5788973.9	Flowing spring		x	Espola (1974)	68	agb16
63	Manupirau springs	Hot springs					43.5	4.9	319.18	445785.4	5789702.7	Flowing spring		x	Espola (1974)	43.5	ajx16
64	Thermal area X	spring 13					53.7	2.1	289.33	445223.3	5789046.8	Flowing spring	1.33	x	Espola (1974)	53.7	aoz16
65	Thermal area X	spring 14					54	2.2	289.02	445220.6	5789055.1	Flowing spring	1.33	x	Espola (1974)	54	aoz16
66	Thermal area X	spring 17					48.5	3.17	289.27	445208.0	5789063.2	Flowing spring	1.33	x	Espola (1974)	48.5	aoz16
67	Thermal area X	spring 27					51	2.5	288.33	445202.5	5789078.2	Flowing spring	1.33	x	Espola (1974)	51	apa16
68	Thermal area X	spring 28					93	6.35	337.57	444610.7	5788286.0	Flowing spring		x	Espola (1974)	93	ki14

ISSN 2703-4275